Organic & Biomolecular Chemistry

PAPER

View Article Online
View Journal | View Issue

Cite this: *Org. Biomol. Chem.*, 2014, **12**, 1652

Identification of BP16 as a non-toxic cell-penetrating peptide with highly efficient drug delivery properties†

Marta Soler,‡[a,b] Marta González-Bártulos,‡[a,c] David Soriano-Castell,[d] Xavi Ribas,[a] Miquel Costas,[a] Francesc Tebar,[d] Anna Massaguer,*[c] Lidia Feliu*[b] and Marta Planas*[b]

Received 4th December 2013,
Accepted 10th January 2014

DOI: 10.1039/c3ob42422g

www.rsc.org/obc

Antimicrobial peptides are an interesting source of non-cytotoxic drug delivery vectors. Herein, we report on the identification of a new cell-penetrating peptide (KKLFKKILKKL-NH_2, **BP16**) from a set of antimicrobial peptides selected from a library of cecropin-melittin hybrids (CECMEL11) previously designed to be used in plant protection. This set of peptides was screened for their cytotoxicity against breast adenocarcinoma MCF-7, pancreas adenocarcinoma CAPAN-1 and mouse embryonic fibroblast 3T3 cell lines. **BP16** resulted to be non-toxic against both malignant and non-malignant cells at concentrations up to 200 μM. We demonstrated by flow cytometry and confocal microscopy that **BP16** is mainly internalized in the cells through a clathrin dependent endocytosis and that it efficiently accumulates in the cell cytoplasm. We confirmed that the cell-penetrating properties of **BP16** are retained after conjugating it to the breast tumor homing peptide CREKA. Furthermore, we assessed the potential of **BP16** as a drug delivery vector by conjugating the anticancer drug chlorambucil to **BP16** and to a CREKA-BP16 conjugate. The efficacy of the drug increased between 6 and 9 times when conjugated to **BP16** and between 2 and 4.5 times when attached to the CREKA-BP16 derivative. The low toxicity and the excellent cell-penetrating properties clearly suggest that **BP16** is a suitable vector for the delivery of therapeutic agents into cells.

Introduction

The efficacy of anticancer treatments remains a key challenge in medicine. Current therapies are hindered by the appearance of toxic side effects and the development of multi-drug resistance by cancer cells.[1,2] Moreover, the use of therapeutic agents is limited by their low permeability through biological membranes. Therefore, there is an actual interest in developing new approaches to cancer treatment.[3] A promising strategy in this area is the use of cell-penetrating peptides (CPPs) as drug delivery systems.[4–9] CPPs are usually short cationic sequences and may be derived from long peptides or proteins present in nature (*i.e.*, Tat peptide or penetratin) or *de novo* designed peptides (*i.e.*, transportan, polyarginine peptides, β-peptides, peptoids, oligocarbamates or polyproline helices).[9–12] The mechanism of action of CPPs initially involves their binding to the negatively charged head groups of lipids or proteins in the plasma membrane which is then followed by their internalization. The exact mode of internalization is still poorly understood but it has been shown to depend on several factors such as the structure and concentration of the CPP as well as the cargo to be transported and the specific cell line.[7,8,12–14] It is believed that endocytosis is the major mode of uptake for CPPs; however, direct translocation can also occur. Due to their ability to cross biomembranes in a non-disruptive way, CPPs offer an opportunity to increase the bioavailability of drugs, enhancing their activity and reducing their dosage. In this sense, CPPs have been described as efficient carriers of nucleic acids, proteins, small molecule drugs and imaging agents.[6–8,10,11,15–18]

Focusing on the idea of obtaining new CPPs with very low toxicity, cationic antimicrobial peptides (AMPs) have emerged as good candidates.[12,19–23] Like CPPs, AMPs are short sequences, containing between 9 and 30 amino acids, and most of them are cationic and amphipathic. These peptides show a broad spectrum of activity against bacteria, fungi, enveloped viruses, parasites, and tumor cells, while exhibiting

[a]*QBIS-CAT Research Group, Institut de Química Computacional i Catàlisi (IQCC) and Departament de Química, Universitat de Girona, Campus Montilivi, E-17071 Girona, Catalonia, Spain*
[b]*LIPPSO, Departament de Química, Universitat de Girona, Campus Montilivi, E-17071 Girona, Catalonia, Spain. E-mail: marta.planas@udg.edu, lidia.feliu@udg.edu; Fax: +34 972418150; Tel: +34 972418274*
[c]*Departament de Biologia, Universitat de Girona, Campus Montilivi, E-17071 Girona, Catalonia, Spain. E-mail: anna.massaguer@udg.edu; Fax: +34 972418150; Tel: +34 972418370*
[d]*Departament de Biologia Cel·lular, Immunologia i Neurociències, Universitat de Barcelona, E-08036 Barcelona, Catalonia, Spain*
†Electronic supplementary information (ESI) available: HPLC, ESI-MS and HRMS of peptides. See DOI: 10.1039/c3ob42422g
‡These authors contributed equally to this work.

low eukaryotic cytotoxicity.[24–31] Several AMPs are being studied for the treatment of human diseases, and some of them have already entered pre-clinical and clinical trials.[26,27] The mechanism of action of AMPs also includes their electrostatic interaction with the negatively charged phospholipid membranes causing morphological changes such as pore formation or cell lysis; however, their translocation into the cytoplasm is not uncommon.[32–35] Due to the latter property, the use of AMPs as CPPs is a field of interest to develop non-cytotoxic delivery vectors. In fact, AMPs, such as LL-37, SynB, melittin and $bLFcin_6$, are able to translocate across human plasma membranes and to act as drug transporters.[36–39]

Binding of a low-molecular-weight drug to a CPP results in an improved uptake, which is associated with a decrease of the dose required to achieve a significant therapeutic effect.[7] In particular, several efforts have been made to conjugate the cytotoxic agent chlorambucil (CLB) to CPPs in order to improve its efficacy.[40–43] Chlorambucil (CLB) is a well-known nitrogen mustard typically used to treat leukemia, but also some breast, lung and ovarian cancers. It is believed that CLB is taken up by passive diffusion and alkylates DNA bringing about its cross-linking.[44] Although this nitrogen mustard is highly effective against certain cancers, its use is limited by the lack of selectivity and the low permeability through cell membranes. To overcome these limitations, CLB has been conjugated to CPPs such as *p*VEC or sC18.[40,41,43]

Despite the high efficiency of CPPs in mediating cellular uptake of pharmacologically active molecules, their use for targeted therapy is limited by their low level of selectivity. Several approaches aimed at improving the specificity of CPPs towards tumor cells have been developed.[45] One of these strategies relies on the conjugation of a CPP with a homing peptide. These peptides bind selectively to overexpressed receptors in human tumor cells providing a means of targeting CPPs towards desired cells or tissues.[46–49] However, most homing peptides have no internalization properties and only can deliver cargos to the cell surface. Thus, homing peptide-CPP conjugates may act as efficient vectors for drug delivery into a specific cell target, improving drug bioavailability, and decreasing side effects and toxicity in healthy cells. An example of a homing peptide is CREKA (Cys-Arg-Glu-Lys-Ala) which was identified by *in vivo* screening of phage-displayed peptide libraries in breast tumors of MMTV-PyMT transgenic mice. CREKA specifically homes to tumors by binding to fibrin and fibrin-associated clotted plasma proteins present in the vessels and the interstitial stroma of tumors.[47,50–52] Since CREKA is not able to internalize cancer cells, it is a good candidate to design peptide-mediated systems for targeted cell delivery of drugs.[41,42]

This study is focused on the search for new CPP candidates and was based on a library of linear undecapeptides (CECMEL11) previously described by Badosa and co-workers to be used for plant protection.[53] This library included sequences highly active against phytopathogenic bacteria and fungi, and low hemolytic activity. Similarly to CPPs, these peptides are cationic and are able to adopt an amphipathic structure. In fact, one member of this library, **BP100**, has been described as an efficient CPP in plant tobacco cells.[54] This background prompted us to study the suitability of peptides from the CECMEL11 library as drug delivery vectors in cancer cells. We first selected several members of this library displaying different antimicrobial and hemolytic activity profiles. Some analogues containing arginine residues were also synthesized and included in the study. The cytotoxicity of these peptides was evaluated in cancer and healthy cell lines. The cellular uptake properties of the peptide with the optimal cytotoxic profile as CPP were then evaluated. We also examined the potential of this CPP candidate as a drug carrier by conjugating it to CLB. In addition, this candidate was conjugated to the homing peptide CREKA to obtain a selective delivery vector for CLB in cancer cells and to confirm that the cell penetrating properties were retained after the incorporation of CREKA and CLB. Thus, we evaluated the cytotoxicity of the CLB-CREKA-CPP conjugate against cancer and healthy cells and its cellular uptake properties.

Results and discussion

Peptide design and synthesis

AMPs represent a source of CPPs because both families share similar structural characteristics. With the aim of identifying new CPPs, we focused our attention on a 125-member library of AMPs (CECMEL11) previously described by Badosa and co-workers.[53] The general structure of this library is $R\text{-}X^1KLFKKILKX^{10}L\text{-}NH_2$, where X^1 and X^{10} correspond to amino acids with various degrees of hydrophobicity and hydrophilicity (Leu, Lys, Phe, Trp, Tyr, Val) and R includes different N-terminal derivatizations (H, Ac, Ts, Bz, Bn). Thus, peptides of this library are highly cationic and their amphipathic character becomes evident when they are represented by means of an Edmunson wheel plot. These structural features have been described as crucial for their antimicrobial activity and also may confer on them cell-penetrating properties.[32–35] In fact, **BP100**, a member of the CECMEL11 library, has been reported as an efficient agent to transport cargoes into plant cells.[54]

In the present study, we examined the ability of sequences of this CECMEL11 library to internalize cancer cells and to transport a drug. Two sets of peptides were considered: (i) undecapeptides **BP16**, **BP76**, **BP81**, **BP100** and **BP105**, and the Arg-containing peptides **BP307** and **BP308**; and (ii) peptide conjugates containing in their structure: the undecapeptide **BP16** and the DNA alkylating agent CLB (**BP325**), **BP16** and the homing peptide CREKA (**BP327**), and **BP16**, CLB and CREKA (**BP329**). To analyze the cellular internalization, **BP16**, **BP325**, **BP327**, and **BP329** were labeled with 5(6)-carboxyfluorescein (CF).

The five peptides of the first set (**BP16**, **BP76**, **BP81**, **BP100** and **BP105**) (Table 1) were selected based on their distinct antibacterial activity against the plant pathogens *Erwinia amylovora*, *Pseudomonas syringae* and *Xanthomonas vesicatoria*, and their different hemolysis percentage at 150 μM.[53] **BP100** and

Table 1 Peptide sequences, retention times and purities on HPLC and HRMS data

Peptide	Sequence[a]	t_R[b] (min)	Purity[c] (%)	HRMS
BP16	KKLFKKILKKL	5.98	87	347.2575 $[M + 4H]^{4+}$, 462.6733 $[M + 3H]^{3+}$
BP76	KKLFKKILKFL	6.40	93	352.0004 $[M + 4H]^{4+}$, 468.9983 $[M + 3H]^{3+}$
BP81	LKLFKKILKFL	6.80	92	348.2477 $[M + 4H]^{4+}$, 463.9946 $[M + 3H]^{3+}$
BP100	KKLFKKILKYL	7.40	100	355.9977 $[M + 4H]^{4+}$, 474.3282 $[M + 3H]^{3+}$
BP105	LKLFKKILKYL	6.65	90	352.2490 $[M + 4H]^{4+}$, 469.3289 $[M + 3H]^{3+}$
BP307	RRLFRRILRYL	7.83	100	391.0091 $[M + 4H]^{4+}$, 521.0091 $[M + 3H]^{3+}$
BP308	RRLFRRILRRL	6.08	99	311.6168 $[M + 5H]^{5+}$, 389.2674 $[M + 4H]^{4+}$
	CREKA	6.63	98	303.1636 $[M + 2H]^{2+}$, 605.3194 $[M + H]^{+}$
BP327	CREKA-KKLFKKILKKL	6.99	95	395.4636 $[M + 5H]^{5+}$, 494.0771 $[M + 4H]^{4+}$
BP325	CLB-KKLFKKILKKL	7.71	91	418.5260 $[M + 4H]^{4+}$, 558.3644 $[M + 3H]^{3+}$
	CLB-CREKA	6.90	90	445.6966 $[M + 2H]^{2+}$, 890.3832 $[M + H]^{+}$
BP329	CLB-CREKA-KKLFKKILKKL	6.92	92	452.4770 $[M + 5H]^{5+}$, 565.3442 $[M + 4H]^{4+}$
CF-BP16	CF-KKLFKKILKKL	6.76, 6.80[d]	93	437.0217 $[M + 4H]^{4+}$, 582.3589 $[M + 3H]^{3+}$
	CF-CREKA	6.25	95	482.1862 $[M + 2H]^{2+}$, 963.3620 $[M + H]^{+}$
BP328	CF-CREKA-KKLFKKILKKL	7.89	97	583.5907 $[M + 4H]^{4+}$, 777.7843 $[M + 3H]^{3+}$
BP326	CLB-KKLFKKILK(CF)KL	7.56	81	677.0473 $[M + 3H]^{3+}$, 1015.0638 $[M + 2H]^{2+}$
BP330	CLB-CREKA-KKLFKKILK(CF)KL	7.53	91	654.8565 $[M + 4H]^{4+}$, 872.8045 $[M + 3H]^{3+}$

[a] All peptides are C-terminal amides. [b] HPLC retention time. [c] Percentage determined by HPLC at 220 nm from the crude reaction mixture. [d] Retention time corresponding to the two isomers of the 5(6)-carboxyfluorescein (CF) labeled peptide.

BP76 are highly active against these phytopathogens (MIC of 2.5 to 7.5 μM) and low hemolytic (22–34%), **BP81** is highly active (MIC of <2.5 to 5 μM) and moderately hemolytic (65%), **BP105** is highly active (MIC of 2.5 to 7.5 μM) and highly hemolytic (91%), and **BP16** is poorly active (MIC > 7.5 μM) and non-hemolytic (0%).

The Arg-containing peptides **BP307** and **BP308** were derived from **BP100** and **BP16**, respectively (Table 1). They were included in this study because most common CPPs, such as Tat or penetratin, are Arg-rich peptides.[55] This residue has been shown to play a key role in peptide internalization due to the hydrogen-bond formation of the guanidino moiety with phosphates, sulfates and carboxylates on cellular components. **BP307** and **BP308** were tested for their antibacterial activity against the above pathogens and for their hemolysis. The replacement of Lys for Arg in **BP16** and **BP100** significantly influenced the antibacterial activity. While **BP307** resulted to be less active (MIC of 6.2 to 12.5 μM) than **BP100**, **BP308** displayed higher antibacterial activity (MIC of 3.1 to 12.5 μM) than **BP16**. In contrast, the hemolysis was not affected and **BP307** and **BP308** exhibited a similar hemolytic activity (28% and 1%, respectively) as the corresponding parent peptide.

Peptide conjugates included in the second set were designed based on **BP16** (Table 1), which showed the best profile as a drug delivery vector among all the above tested undecapeptides (see below). Peptide **BP325** was prepared by coupling CLB to the N-terminus of **BP16** *via* an amide bond. The use of CLB is hampered by its low stability in aqueous environments and its low permeability through biomembranes, limitations that have been overcome by its conjugation to a CPP.[41–44] Moreover, since the use of homing peptides has been described to increase the cell-type specificity of CPPs, **BP327** was designed by conjugating the homing peptide CREKA to the N-terminus of **BP16**. CREKA was selected for its excellent targeting ability to breast tumors and because its linear structure avoids the additional cyclization step required for most other homing peptides. In addition, with the aim of improving the specificity of the cytotoxic agent CLB, **BP329** was synthesized by attaching CLB to CREKA-BP16. Control peptides CREKA and CLB-CREKA were also prepared (Table 1).

These peptides were manually synthesized on a Fmoc-Rink-MBHA resin or on an aminomethyl ChemMatrix resin following a standard Fmoc/*t*Bu strategy and were obtained as C-terminal amides. Couplings of the conveniently protected Fmoc-amino acids and of CLB were mediated by ethyl 2-cyano-2-(hydroxyimino)acetate (Oxyma) and *N*,*N*′-diisopropylcarbodiimide (DIPCDI) in *N*,*N*-dimethylformamide (DMF) or *N*-methyl-2-pyrrolidinone (NMP), depending on the length of the sequence. Peptides were cleaved from the resin by acidolytic treatment and were obtained in excellent purities (87–100%, Table 1), as determined by analytical HPLC. Their identity was confirmed by ESI-MS and HRMS.

On the other hand, **BP16** and **BP327** (CREKA-BP16) were labeled with 5(6)-carboxyfluorescein by coupling this fluorescent label to their N-terminus leading to **CF-BP16** and **BP328**, respectively (Table 1). 5(6)-Carboxyfluorescein labeled CREKA was also prepared (CF-CREKA). Moreover, **BP325** (CLB-BP16) and **BP329** (CLB-CREKA-BP16), incorporating CLB at the N-terminus, were labeled at the side-chain of Lys^9 of the **BP16** fragment, affording **BP326** and **BP330**, respectively. 5(6)-Carboxyfluorescein was introduced using DIPCDI and Oxyma, followed by piperidine washes before cleavage of the peptide from the resin. These washes served to remove overincorporated carboxyfluorescein moieties.[56] For the synthesis of peptides **BP326** (CLB-BP16(CF)) and **BP330** (CLB-CREKA-BP16-(CF)), the lysine residue to be labeled was incorporated as Fmoc-Lys(Dde)-OH. The *N*-[1-(4,4-dimethyl-2,6-dioxocyclohex-1-ylidene)ethyl] (Dde) group was selectively removed by treatment with hydrazine prior to the coupling of the fluorescent label. Acidolytic cleavage afforded the labeled peptides in excellent purities (81–97%), and they were characterized by ESI-MS and HRMS.

Cell cytotoxicity of the CPP candidates

A good CPP to be used as a delivery vector of an anticancer drug must display no toxicity against cancer as well as healthy cells. Hence, the cytotoxicity of undecapeptides **BP16**, **BP76**, **BP81**, **BP100**, **BP105**, **BP307** and **BP308** was screened in breast adenocarcinoma MCF-7 and pancreas adenocarcinoma CAPAN-1 cell lines. The IC_{50} was determined by the 3-(4,5-dimethylthiazol-2-yl)-2,5-diphenyltetrazolium bromide (MTT) assay after 48 h of peptide exposure. As shown in Table 2, except for **BP100**, the undecapeptides were more active against CAPAN-1 than against MCF-7 cells. The cytotoxic activity of **BP76** and **BP105** was significant against these two cell lines, displaying IC_{50} values of 23.5 and 22.7 μM against CAPAN-1, respectively, and of 26.3 and 29.2 μM against MCF-7 cells, respectively. **BP81**, **BP100** and its Arg-containing analogue **BP307** were considerably active against one cell line with IC_{50} values ranging from 24.2 to 35.7 μM. **BP16** and **BP308** were the least cytotoxic undecapeptides. **BP308** showed an IC_{50} of 148.2 and 97.0 μM against MCF-7 and CAPAN-1 cells, respectively, and **BP16** displayed no cytotoxic effects against any of the cancer cell lines tested (IC_{50} > 200 μM).

These results indicate that these undecapeptides exhibit lower cytotoxicity against cancer cells in comparison with their antibacterial activity. However, the structural features that govern the anticancer activity of the CECMEL11 library sequences, **BP16**, **BP76**, **BP81**, **BP100** and **BP105**, correlate with the general trend for the antibacterial activity of this library.[53] Thus, peptides with a net charge of +5 or +6 displayed high cytotoxic activity, whereas **BP16** that has a net charge of +7 was inactive. Moreover, **BP16**, **BP76**, and **BP100** that only differ in the amino acid at position 10 displayed a very distinct cytotoxic activity. The same effect was observed for **BP307** and **BP308**. This result confirms previous data on how subtle changes in a peptide sequence influence the biological activity.[57–59] On the other hand, the replacement of Lys with Arg in **BP16** and **BP100** caused a different effect on the cytotoxicity. While this replacement slightly influenced the cytotoxicity of **BP100**, the Arg-containing sequence **BP308** showed an increased antiproliferative activity compared to **BP16**.

One of the major drawbacks of drug delivery applications of CPPs is their toxicity to normal cells. In this sense, AMPs are interesting CPP candidates because it has been reported that some AMPs with anticancer activity do not show significant cytotoxicity against normal cells at peptide concentrations that are able to kill cancer cells.[19,24,26,28] Parameters that would account for the selective binding of AMPs to cancer cells involves the higher net negative charge and membrane fluidity of cancer cells as compared to normal cells. Therefore, due to their cationic nature, the undecapeptides of this study may preferentially bind to cancer cell membranes by electrostatic interaction and subsequently enter cells.

The analysis of the activity of undecapeptides on non-malignant mouse embryonic fibroblasts 3T3 revealed that the antiproliferative activity of **BP76** and **BP81** was high, with IC_{50} values of 13.5 and 15.5 μM, respectively (Table 2). **BP100**, **BP105**, **BP307** and **BP308** were moderately active (IC_{50} of 39.0 to 68.0 μM). Notably, **BP16** was non-toxic against this cell line exhibiting an IC_{50} > 200 μM. Furthermore, we also used the hemolysis assay to assess the toxicity of these peptides.[53] As mentioned above, except for **BP105** and **BP81**, undecapeptides displayed low hemolysis at 150 μM (0–34%). Interestingly, **BP16** and its Arg analogue **BP308** were nonhemolytic even at 375 μM (data not shown). Even though these undecapeptides did not show selectivity between the malignant and non-malignant cell lines tested, some sequences (**BP76**, **BP100**, and **BP307**) did not show significant hemolytic activity at concentrations much higher than the IC_{50} values against the cancer cell lines tested.

Moreover, the stability in fetal bovine serum of **BP16** was also evaluated and compared to that of Tat_{49}. After exposure to 10% serum at different time intervals, the presence of peptide was analyzed by HPLC. Results showed that both peptides exhibited a similar stability, with 70% degradation after 45 min of incubation.

Taken together, these results allowed the identification of **BP16**, a short and highly cationic peptide with a suitable activity profile to be considered as an excellent CPP candidate. In particular, in contrast to most common CPPs that exhibited cytotoxicity even at low concentrations,[60–63] **BP16** was non-toxic to both malignant and non-malignant cell lines at concentrations up to 200 μM and, therefore, was selected for further studies.

Cellular uptake of BP16

To characterize the capacity of internalization of **BP16** into cancer and non-malignant cells, MCF-7 and 3T3 cells were incubated at 37 °C with 5(6)-carboxyfluorescein labeled **BP16** (**CF-BP16**) at different concentrations (0, 5, 25 and 50 μM) for different times (1, 3 and 6 h) (Fig. 1). The mean fluorescence of the cells, corresponding to the peptide uptake, was

Table 2 Cytotoxicity of the set of undecapeptides in 3T3, MCF-7 and CAPAN-1 cells and their hemolytic activity

	Cell line	BP16	BP76	BP81	BP100	BP105	BP307	BP308
	3T3	>200	13.5 ± 0.7	15.5 ± 0.7	62.5 ± 6.4	39.0 ± 8.5	40.0 ± 7.1	68.0 ± 7.6
IC_{50} [a] (μM)	MCF-7	>200	26.3 ± 7.5	40.0 ± 3.4	34.3 ± 4.0	29.2 ± 4.2	64.7 ± 12.5	148.2 ± 8.8
	CAPAN-1	>200	23.5 ± 7.0	24.2 ± 7.2	57.7 ± 13.3	22.7 ± 1.5	35.7 ± 1.5	97.0 ± 15.4
Hemolysis[b] (%)		0	34 ± 2.1	65 ± 1.5	22 ± 2.8	91 ± 6.2	28 ± 3.2	1 ± 0.1

[a] The IC_{50} values were determined by the MTT assay after 48 h of peptide exposure. Data represent the mean ± SD of at least three independent experiments performed in triplicate. [b] Percent hemolysis at 150 μM. The confidence interval for the mean is included.

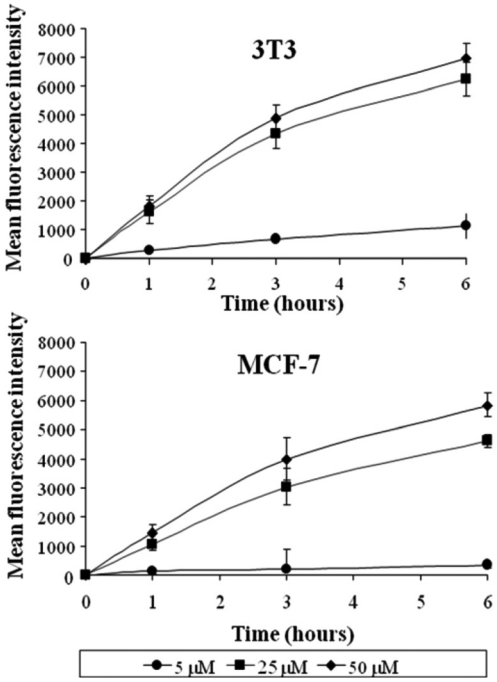

Fig. 1 Kinetics of the cellular uptake of **BP16**. 3T3 and MCF-7 cells were exposed to different concentrations of 5(6)-carboxyfluorescein-labeled **BP16** (**CF-BP16**) (0, 5, 25 and 50 μM) at 37 °C for 1, 3 and 6 h. The fluorescence intensity of the cells, corresponding to the intracellular uptake of the peptide, was determined by flow cytometry. Each point in the graphs represents the mean intracellular fluorescence intensity of three independent experiments + SE.

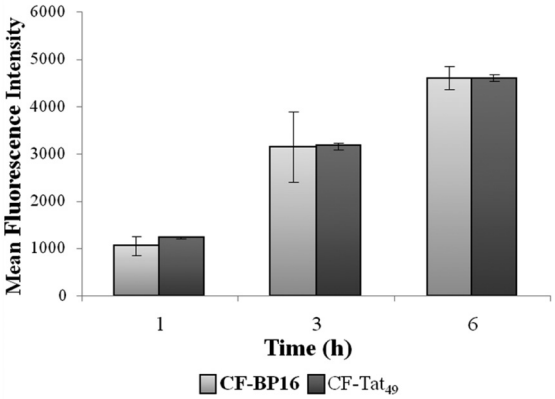

Fig. 2 Uptake of 5(6)-carboxyfluorescein labeled peptides **CF-BP16** and CF-Tat_{49} into MCF-7 cells. Cells were exposed to the peptide at 25 μM at 37 °C for 1, 3 and 6 h. Each column in the graph represents the mean fluorescence intensity of the cells determined in three independent experiments ± SD.

quantified by flow cytometry. Cells were harvested by trypsinization, which also prevented non-specific plasma membrane binding of the peptide. As represented in Fig. 1, **CF-BP16** was efficiently internalized by the cells in a time and concentration-dependent manner. The mean fluorescence of the cells increased over time with parallel internalization kinetics in both cell lines. The cellular uptake of **CF-BP16** was intense during the first 3 h of incubation, particularly when the cells were treated with the peptide at 25 and 50 μM. After treatment with 50 μM **CF-BP16**, the mean fluorescence of 3T3 cells increased from 5 ± 2 (0 h) to 1829 ± 335 (1 h), 4895 ± 464 (3 h) and 6953 ± 536 (6 h), while the mean fluorescence of MCF-7 cells rose from 4 ± 1 (0 h) to 1431 ± 307 (1 h), 3997 ± 720 (3 h) and 5830 ± 410 (6 h). These results point out that the internalization of **CF-BP16** is more elevated in the non-malignant 3T3 cells than in MCF-7 cells, indicating the lack of selectivity of **BP16** for cancer cells.

A good correlation between peptide concentration and its uptake by cells was observed, especially when they were treated with 5 and 25 μM **CF-BP16**. At the different incubation times, when **CF-BP16** concentration was increased from 5 to 25 μM, the mean cellular fluorescence increased by 5 to 6-fold in 3T3 cells and by 8- to 13-fold in MCF-7 cells. In contrast, slight differences in the mean cellular fluorescence (less than 1.7-fold increase) were determined when both cell lines were incubated with **CF-BP16** at 25 or 50 μM, revealing a saturation of the peptide uptake by the cells at concentrations higher than 25 μM.

We compared the capacity of internalization of **BP16** with that of the well-known CPP Tat_{49}.[10] With this aim, MCF-7 cells were incubated at 37 °C with **CF-BP16** and CF-Tat_{49} at 25 μM for 1, 3 and 6 h (Fig. 2). Interestingly, **CF-BP16** and CF-Tat_{49} showed the same mean fluorescence intensity values indicating that **BP16** exhibits an excellent cellular uptake.

To gain more insight into the internalization and intracellular distribution of **BP16**, the cellular uptake of **CF-BP16** was further analyzed by confocal microscopy. For this purpose, MCF-7 cells were incubated with 25 μM **CF-BP16** at 4 °C for 30 min and at 37 °C for 10, 30, 60, 120 and 180 min (Fig. 3A). No fluorescence was observed after 30 min of incubation at 4 °C. However, when the cells were treated at 37 °C, a very faint punctuate fluorescent staining was observed inside the cells after 10 min, revealing an incipient cellular uptake of the peptide. The number of fluorescent particles gradually increased over time and, after 180 min of incubation, there was a prominent fluorescent staining inside the cells, demonstrating intense internalization of the peptide during this period of time. Higher magnification (1000×) images from cells exposed to **CF-BP16** for 180 min (Fig. 3B) revealed that the fluorescent particles were located throughout the whole cytoplasm, with significant clustering at the periphery of the cell nucleus. An optical sectioning indicated that no fluorescence particles were placed inside the cell nucleus (Fig. 3C). In addition, to find out whether **CF-BP16** cellular entry was dependent on specific interaction with the plasma membrane, MCF-7 cells were pre-incubated with 25 μM **CF-BP16** at 4 °C for 30 min and, after extensive washing with saline phosphate buffer, were incubated at 37 °C for 25 min. **CF-BP16** internalization was also compared with the Alexa647-conjugated transferrin (Tf-A647) which is a well-known model of receptor dependent internalized ligands. Confocal images revealed that while transferrin-A647 labelled endocytic structures inside the cell as expected, no intracellular **CF-BP16** was observed

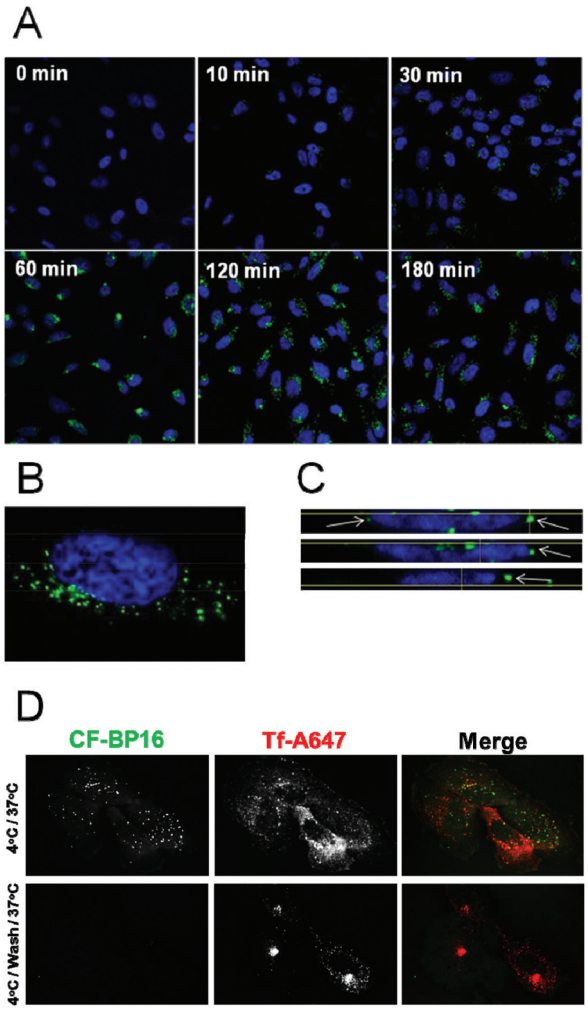

Fig. 3 Confocal microscopic imaging of the internalization of 5(6)-carboxyfluorescein-labeled BP16 (**CF-BP16**) into MCF-7 cells. (A) MCF-7 cells were exposed for 30 min at 4 °C to 25 μM **CF-BP16** and then incubated for the indicated times at 37 °C. The localization of **CF-BP16** is indicated by the green fluorescence. The cell nuclei were stained with Hoeschst (blue). (B) Higher-magnification (1000×) image of a MCF-7 cell after 180 min of treatment. (C) Three slices of a merged *xz* reconstruction of the image stack (slices at 0.3 microns on the *z*-axis) are represented. Arrows indicate the perinuclear localization of **CF-BP16**. (D) MCF-7 cells were pre-incubated for 30 min at 4 °C with 25 μM **CF-BP16** and transferrin-A647 (Tf-A467, 60 μg ml^{-1}) and then incubated for 25 min at 37 °C with or without a previous saline phosphate buffer wash as indicated. Confocal images were acquired through the Alexa647 (red) and CF (green) channels.

(Fig. 3D). This result may indicate the possibility that **CF-BP16** is weakly membrane associated and removed after washes or that **CF-BP16** could be receptor independent and preferentially fluid phase internalized.

These findings highlight a plausible mechanism for the internalization of **BP16**. The mechanism of CPP uptake is controversial and still under debate. Two main pathways have been suggested: endocytosis and direct translocation across the membrane bilayer.[7,8,12–14] These cell uptake phenomena can be related to the hydrophobicity of the CPP. Translocation has been associated with hydrophobic peptides while hydrophilic and amphipathic sequences can be internalized by both mechanisms.[64] In addition, the endocytosis process is energy-dependent and is assumed to be inhibited by peptide incubation at low temperature. Altogether, the results observed for the incubation of **CF-BP16** in MCF-7 cells at 4 and 37 °C suggest that the endocytic pathway may play a major role in **BP16** internalization.

To further characterize the **BP16** endocytosis, the role of dynamin, which is involved in vesicle scission from plasma membrane, was analysed by means of dynamin inhibition using the specific inhibitor dynasore (Fig. 4).[65] The **BP16** endocytosis was also compared with the transferrin protein as a specific marker of a dynamin dependent endocytosis. MCF-7 cells were pre-incubated with 100 μM of dynasore for 15 min at 37 °C and then **CF-BP16** and Tf-A647 were added and further incubated for 60 min. Confocal microscopy images showed an accumulation of Tf-A647 and **CF-BP16** in the same structures at the plasma membrane after dynasore treatment, likely unscissored clathrin coated pits (CCPs) (Fig. 4A). On the other hand, in control cells, **CF-BP16** and

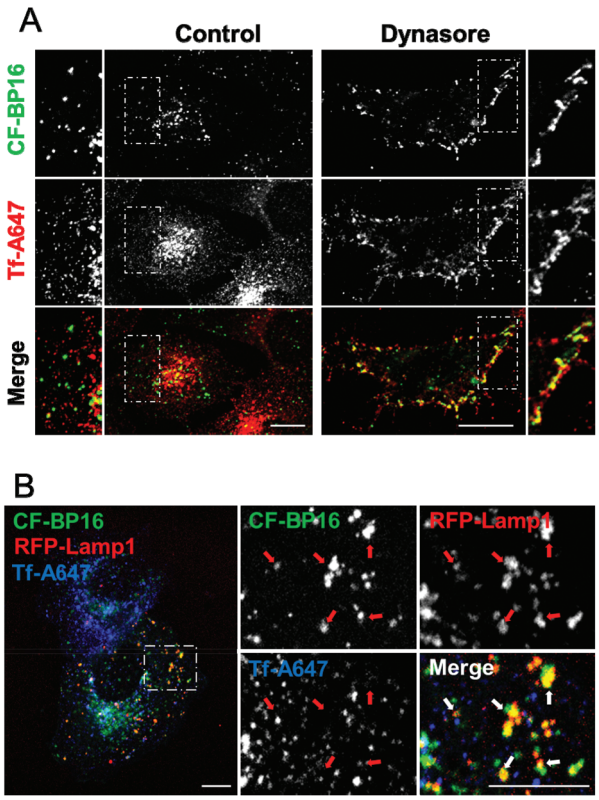

Fig. 4 **CF-BP16** is dynamin dependent internalized, and follows the endocytic degradation pathway. (A) MCF-7 cells were pre-incubated for 15 min at 37 °C with or without 100 μM dynasore and then **CF-BP16** (25 μM) and Alexa647-labelled transferrin (Tf-A647, 60 μg ml^{-1}) were added and further incubated for 60 min. Confocal images were acquired through the Alexa647 (red) and CF (green) channels. (B) MCF-7 cells expressing RFP-Lamp1 (red) were incubated with **CF-BP16** (green) and Tf-A647 (blue) for 60 min at 37 °C. Insets show magnified images and arrows indicate **CF-BP16**/RFP-Lamp1 positive vesicles (bars are 10 μm).

Tf-A647 were found mostly in different endocytic structures inside the cell (Fig. 4A). Indeed, a high degree of co-localization between **CF-BP16** and the ectopically expressed RFP-Lamp1,[66] a marker of late endosomes and lysosomes, was clearly detected (Fig. 4B). These results suggest that CCPs are an important port of entry for **BP16**. However, **BP16** and transferrin follow different endocytic pathways inside the cell, a known recycling pathway for transferrin and a degradation route for **BP16**.

Next, in order to ascertain the importance of clathrin dependent endocytosis (CDE), the role of this dynamin dependent pathway in **CF-BP16** uptake was examined in cells overexpressing the Cherry-DPF fragment of Eps15 protein, which by sequestering AP-2 inhibits CDE (Fig. 5).[67] The **CF-BP16** endocytosis was also compared with the related CF-Tat_{49} peptide and the Tf-A647, which is specifically internalized *via* CDE. Confocal images in Fig. 5 (panels A and B) showed that Tf-A647, **CF-BP16** and CF-Tat_{49} entry was strongly inhibited in those Cherry-DPF overexpressing cells compared to non-expressing cells. In order to quantify such inhibition, internalization of Tf-A647 and **CF-BP16** or CF-Tat_{49} was measured by flow cytometry and compared to dextran-FITC, which enters cells by fluid phase and therefore *via* clathrin dependent and independent pathways. Flow cytometry analysis revealed that transferrin uptake was ~55% inhibited in highly cherry-DPF expressing cells compared to non-transfected cells, while **BP16** and dextran were inhibited by ~47% and ~33%, respectively (Fig. 5C).

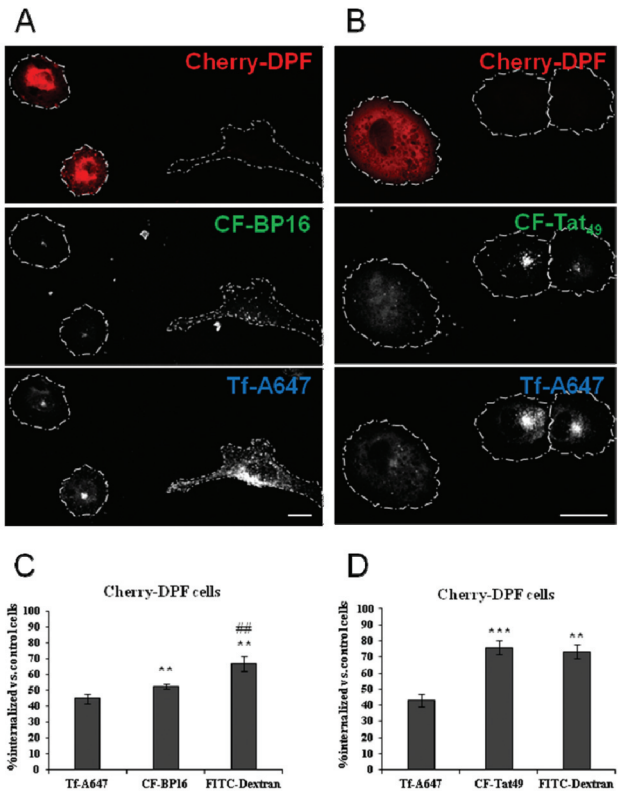

Fig. 5 Clathrin dependent endocytosis is playing a key role in **CF-BP16** uptake. (A, B) Confocal images of MCF-7 cells expressing Cherry-DPF and incubated with Tf-A647 (60 μg ml^{-1}) and **CF-BP16** (25 μM) (A) or CF-Tat_{49} (25 μM) (B) for 60 min at 37 °C (bars are 20 μm). (C, D) Internalization of FITC-dextran (2 mg ml^{-1}), Tf-A647 and **CF-BP16** (C) or CF-Tat_{49} (D) after 60 min at 37 °C was quantified by flow cytometry in Cherry-DPF expressing cells as described in the Experimental section. Histograms show the percentage of the indicated molecules internalized in highly Cherry-DPF expressing cells *versus* non-expressing cells. Each column represents the mean fluorescence intensity of the cells determined in four independent experiments ± SD. Statistical significances between different molecules were determined using the Student's *t*-test, $^{**}p < 0.01$ and $^{***}p < 0.001$ *vs.* Tf-A647; $^{\#\#}p < 0.01$ *vs.* **CF-BP16**.

Given that transferrin endocytosis, which is totally dependent on CDE, was ~55% inhibited and that inhibition of **BP16** was close to transferrin and higher than dextran (~47% *vs.* ~33%), it can be reasoned that CDE is playing a major role in **BP16** internalization. Moreover, flow cytometry inhibition data obtained from Tat_{49} uptake (~19%) compared to dextran (Fig. 5D) suggests that CDE is less important for Tat_{49} internalization than for **BP16**. These results indicate that both peptides, **BP16** and Tat_{49}, are differentially internalized.

In summary, **BP16** internalization is dynamin dependent and it is mainly internalised *via* clathrin dependent endocytosis possibly through a weak plasma membrane interaction or by fluid phase, which is also in agreement with the **BP16** localization in late endosomes after 60 min of endocytosis in MCF-7 cells.

Cell cytotoxicity of peptide conjugates

The potential use of **BP16** as a vector for the delivery of the DNA alkylating agent CLB was assessed by exposing MCF-7, CAPAN-1 and 3T3 cells to CLB and the CLB-BP16 conjugate (**BP325**). The IC_{50} was determined by the MTT assay after 48 h of peptide exposure. As shown in Table 3, CLB alone exhibited low cytotoxicity against the three cell lines (IC_{50} of 73.7 to 152.5 μM). In contrast, **BP325** displayed high activity, with IC_{50} values of 12.0, 13.7 and 20.6 μM against MCF-7, CAPAN-1 and 3T3 cells, respectively. Thus, the conjugation of CLB to **BP16** increased the cell cytotoxicity of this nitrogen mustard by 6-fold in MCF-7 cells, by 7-fold in 3T3 cells and by 9-fold in CAPAN-1 cells. Since **BP16** is non-toxic at these concentrations (IC_{50} > 200 μM), this toxicity must be attributed to the CLB moiety. This increase of activity clearly demonstrates that **BP16** contributes to the internalization of CLB through the cell membrane, enhancing its efficacy. Therefore, in agreement with earlier reports, the mechanism of action of the CLB-BP16 conjugate seems to be much more efficient than the passive diffusion mechanism suggested for CLB alone.[41–44]

Homing peptides are employed to enhance the selectivity of CPPs towards malignant cells.[46–49] Thus, we next investigated whether the cell-penetrating properties of **BP16** were retained after conjugation with the breast tumor homing peptide CREKA and also whether this homing peptide-CPP conjugate could provide selective internalization of CLB into cancer cells. With this aim, the cytotoxicity of the conjugate CLB-CREKA-BP16 (**BP329**) was evaluated in MCF-7, CAPAN-1 and 3T3 cells. CREKA, CLB-CREKA and the conjugate CREKA-BP16

Table 3 Cytotoxicity of **BP16**, CREKA, chlorambucil (CLB), CLB-CREKA, and peptide conjugates in 3T3, MCF-7 and CAPAN-1 cells

	Cell line	**BP16**	CREKA	**BP327**	CLB	CLB-CREKA	**BP325**	**BP329**
IC_{50} [a] (μM)	3T3	>200	>200	74.5 ± 4.1	152.5 ± 5.6	>200	20.6 ± 3.3	33.7 ± 1.9
	MCF-7	>200	>200	74.7 ± 8.8	73.7 ± 4.5	>200	12.0 ± 2.7	35.2 ± 1.8
	CAPAN-1	>200	>200	76.2 ± 0.8	129.0 ± 35.5	>200	13.7 ± 2.4	33.0 ± 1.0

[a] The IC_{50} values were determined by the MTT assay after 48 h of peptide exposure. Data represent the mean ± SD of at least three independent experiments performed in triplicates.

(**BP327**) were also assayed for comparison purposes. CREKA and CLB-CREKA were non-toxic (IC_{50} > 200 μM) and **BP327** displayed low cytotoxicity (IC_{50} of 74.5 to 76.2 μM). In contrast, the conjugate CLB-CREKA-BP16 (**BP329**) was significantly active, with IC_{50} values ranging from 33.0 to 35.2 μM. These results showed that the incorporation of CREKA decreased the activity of the CLB-BP16 conjugate **BP325**; however, they confirmed that **BP16** was able to internalize both CREKA and CLB since the cytotoxicity of **BP329** (CLB-CREKA-BP16) increased 2- to 4.5-fold the one of CLB alone. Furthermore, the lack of selectivity observed for **BP329** could be attributed to the fact that CREKA was originally identified by *in vivo* phage display and recognized fibrin-associated clotted plasma proteins in the tumor stroma.[47,50–52] On this basis, the behavior of CREKA *in vitro* could differ from the one previously described *in vivo*. However, these results show that **BP329** displayed a higher activity than CLB alone proving the validity of **BP16** as CPP for cell delivery of therapeutically useful molecules.

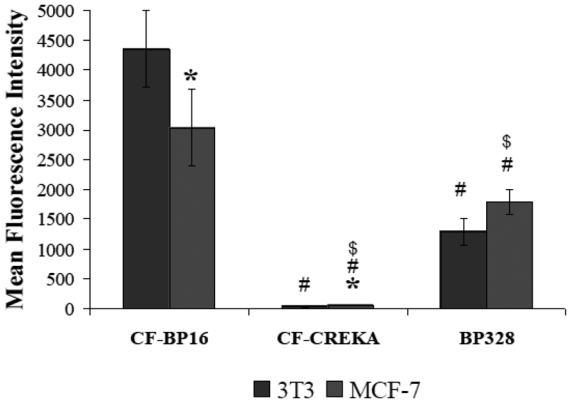

Fig. 6 Uptake of 5(6)-carboxyfluorescein labeled peptides **CF-BP16**, CF-CREKA and **BP328** (CF-CREKA-BP16) into 3T3 and MCF-7 cells. Cells were exposed to the peptides at 25 μM for 3 h at 37 °C. Each column in the graph represents the mean fluorescence intensity of the cells determined in three independent experiments ± SD. *p < 0.05 *vs*. 3T3 cells; #p < 0.05 *vs*. **CF-BP16** treated cells; $$p$ < 0.05 *vs*. CF-CREKA.

Cellular uptake of CLB peptide conjugates

In order to determine whether the differences in cytotoxic activity of the CLB peptide conjugates **BP325** (CLB-BP16) and **BP329** (CLB-CREKA-BP16) were related to their internalization properties, these conjugates were labeled with 5(6)-carboxyfluorescein (CF) affording **BP326** and **BP330**, respectively, and analyzed by flow cytometry. In addition, the homing peptide CREKA and the CREKA-BP16 conjugate (**BP327**) were also labeled (CF-CREKA and **BP328**, respectively) and included in the study.

The cellular uptake of CF-CREKA and **BP328** at 25 μM was determined by flow cytometry after 3 h of incubation in 3T3 and MCF-7 cells at 37 °C. As represented in Fig. 6, very low intracellular fluorescence levels were detected in both cell lines when treated with CF-CREKA, indicating that CREKA alone was unable to internalize into the cells. These results are in accordance with previous studies describing that CREKA displays no cell-penetrating capacity in cultured breast cancer cells.[42] When comparing the fluorescence of **CF-BP16** and **BP328** (CF-CREKA-BP16), it was observed that the cell-penetrating properties of **BP16** were significantly reduced when conjugated to the homing peptide, probably because the coupling of CREKA restricts the interaction of **BP16** with the cell membrane. Notably, as shown by the intracellular fluorescence levels, **BP328** retains significant internalization ability which is required to deliver cytotoxic agents inside the cells.

The internalization ability of the CLB peptide conjugates **BP326** (CLB-BP16(CF)) and **BP330** (CLB-CREKA-BP16(CF)) at 25 μM was evaluated by flow cytometry in MCF-7 cells after 3 h of incubation at 37 °C. To our surprise, while the fluorescence of **BP326** (4272 ± 453) was not significantly different from that of **CF-BP16** (3035 ± 643), **BP330** showed a considerably higher intracellular fluorescence (3966 ± 217) than **BP328** (CF-CREKA-BP16) (1789 ± 221). These results are noteworthy since they prove that **BP16** is able to efficiently internalize both CLB and CREKA.

These findings also reveal that the incorporation of either CREKA and/or CLB has a strong influence on the cellular uptake of **BP16**, reflecting that any modification in the molecular structure of this peptide can lead to relevant changes in its cell penetrating properties. In fact, it has been reported that the cargo plays an important role in the internalization mechanism of CPPs.[8,11] Interestingly, despite these modifications, **BP16** remains an efficient drug delivery vector.

Conclusions

In the present study, we have identified **BP16** as a new CPP with high cellular uptake *in vitro*. In contrast to other CPPs previously reported, **BP16** displays no cytotoxicity against malignant and non-malignant cells and, moreover, shows no

hemolytic activity. We have demonstrated that **BP16** exhibits highly efficient penetration through endocytic mechanisms, accumulating in the cell cytoplasm at short time periods. In addition, the conjugation of the DNA alkylating agent CLB to **BP16** dramatically increases the cytotoxicity of this drug between 6- and 9-fold. We have also shown that, in conjugation with the homing peptide CREKA, **BP16** is able to improve the cytotoxic activity of CLB from 2- to 4.5-fold. Taken together, these results confirm that **BP16** is an excellent non-toxic delivery vector suitable for the effective transport of drugs. Further studies on applications of this CPP are underway in our laboratory.

Experimental section

Materials and methods

Unless otherwise stated, common chemicals and solvents (HPLC-grade or reagent-grade quality) were purchased from commercial sources and used without further purification. The 9-fluorenylmethoxycarbonyl (Fmoc) derivatives and Fmoc-Rink-4-methylbenzhydrylamine (MBHA) resin (0.56 mmol g^{-1}) were obtained from Senn Chemicals International (Gentilly, France), NovaBiochem (Schwalbach, Germany) or from IRIS Biotech GmbH (Marktredwitz, Germany). Aminomethyl ChemMatrix resin (0.66 mmol g^{-1}) was obtained from Matrix Innovation Inc (St-Hubert, Canada). Ethyl 2-cyano-2-(hydroxyimino) acetate (Oxyma) was purchased from Novabiochem (Nottingham, UK). Trifluoroacetic acid (TFA), triisopropylsilane (TIS), dimethyl sulfoxide (DMSO), D,L-dithiothreitol (DTT), *N*,*N*′-diisopropylcarbodiimide (DIPCDI), chlorambucil (CLB), 5(6)-carboxyfluorescein (CF), fluorescein isothiocyanate dextran mol. wt 10 000 (FITC-dextran) and dynasore hydrate were from Sigma-Aldrich (St. Louis, MO, USA). Transferrin Alexa Fluor® 647 conjugate was from Molecular Probes (Invitrogen, Life Technologies, Carlsbad, CA). Piperidine was purchased from Fluka (Buchs, Switzerland). *N*-Methyl-2-pyrrolidinone (NMP), *N*,*N*-dimethylformamide (DMF), CH_3OH, CH_2Cl_2, diethyl ether and solvents for high performance liquid chromatography (HPLC) were obtained from Scharlau (Sentmenat, Spain).

3-(4,5-Dimethylthiazol-2-yl)-2,5-diphenyltetrazolium bromide (MTT), paraformaldehyde, and bisbenzimide trihydrochloroacetic acid (Hoechst 33258) were purchased from Sigma-Aldrich (St. Louis, MO, USA). Dulbecco's modified Eagle's medium (DMEM), phosphate buffered saline (PBS), fetal bovine serum (FBS), penicillin–streptomycin and trypsin were obtained from GIBCO BRL (Grand Island, NY, USA). The RFP-Lamp1 plasmid was kindly provided by Walther Mothes (Addgene plasmid 1817).[66]

Electrospray ionization mass spectrometry (ESI-MS) analyses were performed with an Esquire 6000 ESI ion trap LC/MS (Bruker Daltonics) instrument equipped with an electrospray ion source. The instrument was operated in the positive ESI(+) ion mode (University of Girona). Samples (5 μL) were introduced into the mass spectrometer ion source directly through an HPLC autosampler. The mobile phase (80 : 20 CH_3CN–H_2O at a flow rate of 100 μL min^{-1}) was delivered by a 1100 Series HPLC pump (Agilent). Nitrogen was employed as both the drying and nebulizing gas.

High-resolution mass spectra (HRMS) were recorded under conditions of ESI with a Bruker MicrOTOF-Q IITM instrument using a hybrid quadrupole time-of-flight mass spectrometer (University of Girona). Samples were introduced into the mass spectrometer ion source by direct infusion through a syringe pump and were externally calibrated using sodium formate. The instrument was operated in the positive ESI(+) ion mode.

Cell lines

The human breast cancer cell line MCF-7, the human pancreas cancer cell line CAPAN-1 and the mouse fibroblast cell line 3T3 were obtained from the American Tissue Culture Collection (ATCC, Rockville, MD, USA). Cells were maintained in DMEM supplemented with 10% FBS and 100 U ml^{-1} penicillin–streptomycin at 37 °C under a humidified atmosphere containing 5% CO_2. Cells were passaged two times per week.

Peptide synthesis

General method for solid-phase peptide synthesis. Peptides from Table 1, Tat_{49} and CF-Tat_{49}, were synthesized manually by the solid-phase method using Fmoc-type chemistry and the following side-chain protecting groups: *tert*-butyloxycarbonyl (Boc) for Lys, *t*Bu for Tyr and Glu, trityl (Tr) for Cys, and 2,2,5,7,8-pentamethylchroman-6-sulphonyl (Pmc) for Arg. A Fmoc-Rink-MBHA resin (0.56 mmol g^{-1}) or an aminomethyl ChemMatrix resin (0.66 mmol g^{-1}) were used as a solid support to obtain peptide amides. Coupling of Fmoc-Rink (4 equiv.) onto the aminomethyl ChemMatrix resin was mediated by DIPCDI (4 equiv.) and Oxyma (4 equiv.) in DMF at room temperature overnight. Couplings of the Fmoc-amino acids (4 equiv.) were performed using DIPCDI (4 equiv.) and Oxyma (4 equiv.) in DMF under stirring at room temperature for 2 h, and monitored by the Kaiser test.[68] For sequences containing up to eleven residues, the Fmoc group was removed by treating the resin with a mixture of piperidine–DMF (3 : 7, 1 × 2 min + 1 × 10 min). For longer sequences, Fmoc group removal was carried out with piperidine–DMF (3 : 7, 1 × 3 min + 3 × 10 min). After each coupling and deprotection step, the resin was washed with DMF (6 × 1 min) and CH_2Cl_2 (6 × 1 min), and air-dried. After the coupling of the eleventh residue, NMP was used instead of DMF. Peptide elongation was performed by repeated cycles of Fmoc group removal, coupling and washings.

Once the synthesis was completed, peptidyl resins were subjected to the N-terminal Fmoc group removal. Then, peptides were cleaved or the peptidyl resins were derivatized with CLB and/or with 5(6)-carboxyfluorescein. Cleavage of peptides from the resin was performed by treatment with TFA–TIS–H_2O (95 : 2.5 : 2.5) for 3 h at room temperature. Peptides containing a cysteine residue were cleaved with TFA–TIS–H_2O–DTT (92.5 : 2.5 : 2.5 : 2.5) for 3 h at room temperature. Both procedures were followed by TFA evaporation by bubbling N_2 into the solution. Crude peptides were precipitated by adding cold

diethyl ether (−20 °C) and collected by centrifugation. This procedure was repeated twice. Finally, peptides were dissolved in H_2O–CH_3CN (50 : 50 v/v containing 0.1% TFA), lyophilized and tested for purity by HPLC. Analysis was carried out with a Kromasil C18 reverse-phase column (4.6 × 40 mm; 3.5 μm particle size) with a 2–100% B linear gradient over 7 min at a flow rate of 1.0 ml min^{-1}. Solvent A was 0.1% aqueous TFA and solvent B was 0.1% TFA in CH_3CN. Detection was performed at 220 nm. ESI-MS and HRMS (ESI) were used to confirm peptide identity. Peptides from Table 1, Tat_{49} and CF-Tat_{49}, were obtained in purities ranging from 81 to 100%.

Synthesis of CLB-peptide conjugates. Derivatization with CLB was performed by treating the corresponding peptidyl resin with CLB (5 equiv.), DIPCDI (5 equiv.) and Oxyma (5 equiv.) in DMF or NMP under stirring at room temperature for 5 h. The completion of the reaction was checked by the Kaiser test.[68] The resin was then washed with NMP (6 × 1 min), CH_3OH (6 × 1 min), and CH_2Cl_2 (6 × 1 min), and air dried.

Synthesis of N-terminal 5(6)-carboxyfluorescein-labeled peptides. For the N-terminal derivatization with 5(6)-carboxyfluorescein, this fluorophore (2.5 equiv.) was first pre-activated with Oxyma (2.5 equiv.) and DIPCDI (2.5 equiv.) in CH_2Cl_2–NMP (1 : 9) for 10 min. The mixture was added to the corresponding N-terminal deprotected peptidyl resin and reacted overnight at room temperature protected from light by covering it with aluminum foil due to the light sensitivity of 5(6)-carboxyfluorescein. Completeness of the coupling was confirmed using the Kaiser test.[68] The resin was then washed with NMP (1 × 5 min), piperidine–NMP (1 : 5, 1 × 15 min), NMP (6 × 1 min), CH_2Cl_2 (6 × 1 min), CH_3OH (6 × 1 min), and CH_2Cl_2 (6 × 1 min) and air dried.[56]

Synthesis of 5(6)-carboxyfluorescein-labeled CLB-peptide conjugates. These conjugates were prepared from a peptidyl resin incorporating the lysine residue to be labeled protected with *N*-[1-(4,4-dimethyl-2,6-dioxocyclohex-1-ylidene)ethyl] (Dde) at the N^{ε}-amino group. After CLB coupling, the Dde group was removed by treatment with hydrazine–NMP (2 : 98, 5 × 20 min) under stirring at room temperature and the deprotection progress was monitored by the Kaiser test.[68] Then, the resin was washed with NMP (6 × 1 min) and CH_2Cl_2 (6 × 1 min) and air dried. Next, fluorophore labeling with 5(6)-carboxyfluorescein was carried out as described for the N-terminal carboxyfluorescein labeled peptides.

Cytotoxicity assays

Cytotoxicity of peptides **BP16**, **BP76**, **BP81**, **BP100**, **BP105**, **BP307**, **BP308**, CREKA and **BP327**, CLB-peptide conjugates CLB-CREKA, **BP325** and **BP329**, and CLB in 3T3, MCF-7 and CAPAN-1 cells was determined by the MTT assay. Peptides and CLB-peptide conjugates were diluted in Milli-Q water to obtain 2 mM stock solutions. CLB was dissolved in DMSO to provide a 75 mM stock solution.[69] Appropriate aliquots of these solutions were diluted in the cell culture medium to obtain the final working concentrations. Aliquots of 4000 3T3 cells, 6000 MCF-7 cells or 10 000 CAPAN-1 cells were seeded on 96-well plates 24 h prior to the treatments. Then, cells were treated for 48 h with the corresponding compound at concentrations ranging from 0 to 200 μM. After removal of the treatment, cells were washed with PBS and incubated for an additional 2 h in the dark with fresh culture medium (100 μL) with MTT (10 μL). The medium was discarded and DMSO (100 μL) was added to each well to dissolve the purple formazan crystals. Plates were agitated at room temperature for 10 min and the absorbance of each well was determined with an absorbance microplate reader (ELx800, BioTek, Winooski, USA) at a wavelength of 570 nm. Three replicates for each compound were used, and all treatments were tested at least in three independent experiments. For each treatment, the cell viability was determined as a percentage of the control untreated cells by dividing the mean absorbance of each treatment by the mean absorbance of the untreated cells. The concentration that reduces by 50% the cell viability (IC_{50}) was established for each compound.

Hemolysis

The data corresponding to the hemolytic activity of peptides were previously reported by Badosa *et al.*[53] It was evaluated at 150 μM by determining the hemoglobin release from erythrocyte suspensions of fresh human blood (5% v/v) using absorbance at 540 nm.

Stability of BP16 and Tat_{49} in serum

The stability of **BP16** and Tat_{49} was evaluated in fetal bovine serum. Each peptide (1 mg) was exposed to 10% aqueous filtered fetal bovine serum (2 ml) at 37 °C. After 5, 10, 15, 30 and 45 min exposure, aliquots (200 μL) were removed and proteins were precipitated with CH_3CN (200 μL). Samples were cooled to 0 °C for 15 min and centrifuged (11 000 rpm, 5 min). The supernatant was analyzed by HPLC. The digestion was estimated as the percentage of degraded peptide calculated from the decrease of the HPLC peak area of the native peptide.

Flow cytometry

The uptake efficiency of **CF-BP16**, CF-CREKA, and **BP328** by 3T3 and MCF-7 cells and of CF-Tat_{49}, **BP326**, and **BP330** by MCF-7 cells was quantified by flow cytometry. Aliquots of 50 000 cells were seeded in 24 well plates and allowed to attach for 24 h. Next, the cells were incubated with **CF-BP16** at 5, 25 and 50 μM for 1, 3 and 6 h, with CF-CREKA, **BP328**, **BP326** and **BP330** at 25 μM for 3 h or with **CF-BP16** and CF-Tat_{49} at 25 μM for 1, 3 and 6 h at 37 °C. The cells were harvested by trypsinization and gently washed with 2% FBS in cold PBS. The fluorescence of the cells, corresponding to the cellular uptake of the carboxyfluorescein labeled peptides, was analyzed using a FACSCalibur (Becton Dickinson Immunocytometry Systems, San Jose, CA) equipped with the CellQuestTM software (Becton Dickinson). The mean fluorescence intensity was represented on a four orders of magnitude log scale (1–10 000). The effect of Cherry-DPF expression on **CF-BP16**, CF-Tat_{49}, transferrin-A647 and FITC-Dextran uptake in MCF-7 cells was also analysed by flow cytometry. MCF-7 cells seeded in 6 well plates

were transfected with Cherry-DPF plasmid using Effectene (Qiagen, Hiden, Germany) according to the manufacturer's specifications. To generate the Cherry-DPF plasmid, the DPF fragment (aa_s: 501–874) from human Eps15 was obtained by polymerase chain reaction and cloned into pEGFP-C1 vector (Clontech) using XhoI and Pst1 restriction sites and after that GFP was replaced with the mCherry fluorescent protein. After 24 h of protein expression, cells were incubated with transferrin-A647 (60 μg ml^{-1}) combined with **CF-BP16** (25 μM), CF-Tat_{49} (25 μM) or FITC-Dextran (2 mg ml^{-1}) for 60 min at 37 °C and washed two times with cold PBS. The remaining fluorescence at the cell surface was removed by a 3 min cold acid wash (0.2 M sodium acetate, 0.5 M sodium chloride, pH 4.5) and the intracellular fluorescence was quantified using a LSRFortessa (Becton Dickinson) equipped with the CellQuestTM software (Becton Dickinson). Ten thousand cells were analyzed in each experiment.

Confocal microscopy

MCF-7 cells grown on coverslips and incubated with different fluorescent-labeled molecules were washed with cold PBS and fixed with freshly prepared 4% paraformaldehyde in PBS for 15 min at 4 °C. After washing twice with PBS, the coverslips were mounted in Mowiol (Calbiochem, Merck, KGaA, Darmstadt, Germany) or using a fluorescence mounting medium (Dako, Carpinteria, CA, USA). The images were acquired using a Leica TCS SP5 laser scanning confocal microscope (Leica Microsystems Heidelberg GmbH) equipped with a DMI6000 inverted microscope, blue diode (405 nm), argon (458/476/488/514), diode pumped solid state (561 nm) and HeNe (633) lasers. Final imaging was performed using ImageJ software.

Statistical analysis

The statistical analysis was performed with the SPSS statistical software for Windows (version 15.0; SPSS Inc., Chicago, IL, USA). Quantitative variables were expressed as mean and standard deviation (SD). The normality of the data was tested using the Shapiro–Wilk test. The differences between data with normal distribution and homogeneous variances were analyzed using the parametric Student's t test. A value of $p < 0.05$ was considered significant.

Acknowledgements

This work was supported by Consolider Ingenio CSD/CSD2010-00065 from MICINN of Spain and by grant BFU2012-38259 from Ministerio de Economia y Competitividad of Spain to F.T. We also thank the Catalan DIUE of the Generalitat de Catalunya (2009SGR637). X.R. thanks financial support from INNPLANTA project INP-2011-0059-PCT-420000-ACT1. M.C. and X.R. thank ICREA Academia Awards. D.S.-C. is a recipient of FI fellowship (Generalitat de Catalunya). We also acknowledge the Serveis Tècnics de Recerca of the University of Girona for technical support.

Notes and references

1 D. Hanahan and R. A. Weinberg, *Cell*, 2011, **144**, 646–674.
2 C. H. Takimoto and E. Calvo, in *Cancer Management: A Multidisciplinary Approach*, ed. R. Pazdur, L. D. Wagman, K. A. Camphausen, W. J. Hoskins, UBM Medica, London, 2008, pp. 42–58.
3 E. Raschi, V. Vasina, M. G. Ursino, G. Boriani, A. Martoni and F. De Ponti, *Pharmacol. Ther.*, 2010, **125**, 196–218.
4 E. L. Snyder and S. F. Dowdy, *Pharm. Res.*, 2004, **21**, 389–393.
5 E. Vivès, J. Schmidt and A. Pèlegrin, *Biochim. Biophys. Acta*, 2008, **1786**, 126–138.
6 K. M. Stewart, K. L. Horton and S. O. Kelly, *Org. Biomol. Chem.*, 2008, **6**, 2242–2255.
7 S. B. Fonseca, M. P. Pereira and S. O. Kelley, *Adv. Drug Delivery Rev.*, 2009, **61**, 953–964.
8 E. Koren and V. P. Torchilin, *Trends Mol. Med.*, 2012, **18**, 385–393.
9 F. Milleti, *Drug Discovery Today*, 2012, **17**, 850–860.
10 J. S. Wadia and S. F. Dowdy, *Adv. Drug Delivery Rev.*, 2005, **57**, 579–596.
11 V. Kersemans, K. Kersemans and B. Cornelissen, *Curr. Pharm. Des.*, 2008, **14**, 2415–2427.
12 R. Fischer, M. Fotin-Mleczek, H. Hufnagel and R. Brock, *ChemBioChem*, 2005, **6**, 2126–2142.
13 S. Pujals, J. Fernández-Carneado, C. López-Iglesias, M. J. Kogan and E. Giralt, *Biochim. Biophys. Acta*, 2006, **1758**, 264–279.
14 P. Lundberg and U. Langel, *J. Mol. Recognit.*, 2003, **16**, 227–233.
15 M. Gooding, L. P. Browne, F. M. Quinteiro and D. L. Selwood, *Chem. Biol. Drug Des.*, 2012, **80**, 787–809.
16 S. A. Nasrollahi, C. Taghibiglou, E. Azizi and E. S. Farboud, *Chem. Biol. Drug Des.*, 2012, **80**, 639–646.
17 T. Lehto, K. Kurrikoff and U. Langel, *Expert Opin. Drug Deliv.*, 2012, **9**, 823–836.
18 I. Nakase, H. Akita, K. Kogure, A. Gräslund, U. Langel, H. Harashima and S. Futaki, *Acc. Chem. Res.*, 2012, **45**, 1132–1139.
19 F. Schweizer, *Eur. J. Pharmacol.*, 2009, **625**, 190–194.
20 Y. Li, Q. Xiang, Q. Zhang, Y. Huang and Z. Su, *Peptides*, 2012, **37**, 207–215.
21 K. Takeshima, A. Chikushi, K.-K. Lee, S. Yonehara and K. Matsuzako, *J. Biol. Chem.*, 2003, **278**, 1310–1315.
22 S. T. Henriques, M. N. Melo and M. A. R. B. Castanho, *Biochem. J.*, 2006, **399**, 1–7.
23 J. Fernández-Carneado, M. J. Kogan, S. Pujals and E. Giralt, *Biopolymers*, 2004, **76**, 196–203.
24 C. Leuschner and W. Hansel, *Curr. Pharm. Des.*, 2004, **10**, 2299–2310.
25 C. D. Fjell, J. A. Hiss, R. E. W. Hancock and G. Schneider, *Nat. Rev. Drug Discovery*, 2012, **11**, 37–51.
26 D. W. Hoskin and A. Ramanoorthy, *Biochim. Biophys. Acta*, 2008, **1778**, 357–375.
27 E. Randal, *Future Microbiol.*, 2011, **6**, 635–666.

28 J. S. Mader and D. W. Hoskin, *Expert Opin. Invest. Drugs*, 2006, **15**, 933–946.
29 P. Bulet, R. Stöcklin and L. Menin, *Immunol. Rev.*, 2004, **198**, 169–184.
30 H. Jenssen, P. Hamill and R. E. W. Hancock, *Clin. Microbiol. Rev.*, 2006, **19**, 491–511.
31 M. Zasloff, *Nature*, 2002, **415**, 389–395.
32 B. Bechinger and K. Lohner, *Biochim. Biophys. Acta*, 2006, **1758**, 1529–1539.
33 R. E. W. Hancock and H. G. Sahl, *Nat. Biotechnol.*, 2006, **24**, 1551–1557.
34 J. F. Marcos and M. Gandía, *Expert Opin. Drug Discov.*, 2009, **4**, 659–671.
35 H. W. Huang, *Biochim. Biophys. Acta*, 2006, **1758**, 1292–1302.
36 B. Fang, H. Y. Guo, M. Zhang, L. Jiang and F. Z. Ren, *FEBS J.*, 2013, **280**, 1007–1017.
37 G. Drin, S. Cottin, E. Blanc, A. R. Rees and J. Temsamani, *J. Biol. Chem.*, 2003, **278**, 31192–31201.
38 K. K. Hou, H. Pan, G. M. Lanza and S. A. Wickline, *Biomaterials*, 2013, **34**, 3110–3119.
39 S. Sandgren, A. Wittrup, F. Cheng, M. Jönsson, E. Eklund, S. Busch and M. Belting, *J. Biol. Chem.*, 2004, **279**, 17951–17956.
40 H. Myrberg, L. Zhang, M. Mäe and U. Langel, *Bioconjugate Chem.*, 2008, **19**, 70–75.
41 M. Mäe, H. Myrberg, S. El-Andaloussi and U. Langel, *Int. J. Pept. Res. Ther.*, 2009, **15**, 11–15.
42 S. B. Fonseca and S. O. Kelley, *ACS Med. Chem. Lett.*, 2011, **2**, 419–423.
43 J. Hoyer, U. Schatzschneider, M. Schulz-Siegmund and I. Neundorf, *Beilstein J. Org. Chem.*, 2012, **8**, 1788–1797.
44 S. R. Rajski and R. M. Williams, *Chem. Rev.*, 1998, **98**, 2723–2795.
45 I. Martín, M. Teixidó and E. Giralt, *Pharmaceuticals*, 2010, **3**, 1456–1490.
46 S. Majumdar and T. J. Siahaan, *Med. Res. Rev.*, 2012, **32**, 637–658.
47 N. Svensen, J. G. A. Walton and M. Bradley, *Trends Pharmacol. Sci.*, 2012, **33**, 186–192.
48 P. Laakkonen and K. Vuorinen, *Integr. Biol.*, 2010, **2**, 326–337.
49 O. H. Aina, R. Liu, J. L. Sutcliffe, J. Marik, C.-X. Pan and K. S. Lam, *Mol. Pharmaceutics*, 2007, **4**, 631–651.
50 D. Simberg, T. Duza, J. H. Park, M. Essler, J. Pilch, L. Zhang, A. M. Derfus, M. Yang, R. M. Hoffman, S. Bhatia, M. J. Sailor and E. Ruoslahti, *Proc. Natl. Acad. Sci. U. S. A.*, 2007, **104**, 932–936.
51 E. H. M. Lempens, M. Merkx, M. Tirrel and E. W. Meijer, *Bioconjugate Chem.*, 2011, **22**, 397–405.
52 W. Qu, W. H. Chen, Y. Kuang, X. Zeng, S. X. Cheng, X. Zhou, R. X. Zhuo and X. Z. Zhang, *Mol. Pharmaceutics*, 2013, **10**, 261–269.
53 E. Badosa, R. Ferre, M. Planas, L. Feliu, E. Besalú, J. Cabrefiga, E. Bardají and E. Montesinos, *Peptides*, 2007, **28**, 2276–2285.
54 K. Eggenberger, C. Mink, P. Wadhwani, A. S. Ulrich and P. Nick, *ChemBioChem*, 2011, **12**, 132–137.
55 K. Melikov and L. V. Chernomordik, *Cell. Mol. Life Sci.*, 2005, **62**, 2739–2749.
56 R. Fischer, O. Mader, G. Jung and R. Brock, *Bioconjugate Chem.*, 2003, **14**, 653–660.
57 I. Güell, J. Cabrefiga, E. Badosa, R. Ferre, M. Talleda, E. Bardají, M. Planas, L. Feliu and E. Montesinos, *Appl. Environ. Microbiol.*, 2011, **77**, 2667–2675.
58 S. Monroc, E. Badosa, E. Besalú, M. Planas, E. Bardají, E. Montesinos and L. Feliu, *Peptides*, 2006, **27**, 2575–2584.
59 E. Badosa, R. Ferre, J. Francés, E. Bardají, L. Feliu, M. Planas and E. Montesinos, *Appl. Environ. Microbiol.*, 2009, **75**, 5563–5569.
60 S. Aroui, S. Brahim, M. De Waard and A. Kenani, *Biochem. Biophys. Res. Commun.*, 2010, **391**, 419–425.
61 H. Yang, S. Liu, H. Cai, L. Wan, S. Li, Y. Li, J. Cheng and X. Lu, *J. Biol. Chem.*, 2010, **285**, 25666–25676.
62 J. Song, M. Kai, W. Zhang, J. Zhang, L. Liu, B. Zhang, X. Liu and R. Wang, *Peptides*, 2011, **32**, 1934–1941.
63 S. Jones and J. Howl, *Bioconjugate Chem.*, 2012, **23**, 47–56.
64 J. Farrera-Sinfreu, E. Giralt, S. Castel, A. Albericio and M. Royo, *J. Am. Chem. Soc.*, 2005, **127**, 9459–9468.
65 E. Macia, M. Ehrlich, R. Massol, E. Boucrot, C. Brunner and T. Kirchhausen, *Dev. Cell.*, 2006, **10**, 839–850.
66 N. M. Sherer, M. J. Lehmann, L. F. Jimenez-Soto, A. Ingmundson, S. M. Horner, G. Cicchetti, P. G. Allen, M. Pypaert, J. M. Cunningham and W. Mothes, *Traffic*, 2003, **4**, 785–801.
67 A. Benmerah, C. Lamaze, B. Bègue, S. L. Schmid, A. Dautry-Varsat and N. Cerf-Bensussan, *J. Cell Biol.*, 1998, **140**, 1055–1062.
68 E. Kaiser, R. L. Colescott, C. D. Bossinger and P. Cook, *Anal. Biochem.*, 1970, **34**, 595–598.
69 A. Guaragna, A. Chiaviello, C. Paolella, D. D'Alonzo, G. Palumbo and G. Palumbo, *Bioconjugate Chem.*, 2012, **23**, 84–96.